



CHORUS

This is the accepted manuscript made available via CHORUS. The article has been published as:

Impact of nuclear spin dynamics on electron transport through donors

S. K. Gorman, M. A. Broome, W. J. Baker, and M. Y. Simmons

Phys. Rev. B **92**, 125413 — Published 10 September 2015

DOI: [10.1103/PhysRevB.92.125413](https://doi.org/10.1103/PhysRevB.92.125413)

The impact of nuclear spin dynamics on electron transport through donors

S. K. Gorman, M. A. Broome, W. J. Baker, M. Y. Simmons

*Centre of Excellence for Quantum Computation and Communication Technology,
School of Physics, University of New South Wales, Sydney, New South Wales 2052, Australia*

(Dated: July 31, 2015)

We present an analysis of electron transport through two weakly coupled precision placed phosphorus donors in silicon. In particular, we examine the $(1,1)\leftrightarrow(0,2)$ charge transition where we predict a new type of current blockade driven entirely by the nuclear spin dynamics. Using this nuclear spin blockade mechanism we devise a protocol to readout the state of single nuclear spins using electron transport measurements only. We extend our model to include realistic effects such as Stark shifted hyperfine interactions and multi-donor clusters. In the case of multi-donor clusters we show how nuclear spin blockade can be alleviated allowing for low magnetic field electron spin measurements.

PACS numbers: 85.35.Gv, 73.23.Hk, 87.15.hj, 76.30.-v

I. INTRODUCTION

An understanding of electron transport through multiple quantum dots has enabled the progression of semiconductor quantum information protocols from single shot spin readout to two-qubit logic gates¹⁻⁴. Not only do transport measurements provide us with important details on spin relaxation times and tunnel rates, but they play a vital role in aiding our understanding of the complex spin dynamics that occur in these systems, such as coherent manipulation of the electron spins^{2,5} and dynamical nuclear polarisation of the Overhauser field⁶.

With recent advances in the fabrication of precision placed donors in silicon⁷⁻¹¹ research in this field is now focused on spin transport through multi-donor chains. A deeper understanding of the interplay between electron- and nuclear-spins in the dynamics of such systems is a prerequisite for the progression of this field. In particular for the implementation of spin transport via donor chains¹². So far, protocols based on spin-chains¹³⁻¹⁵, coherent tunneling adiabatic passage (CTAP)^{12,16,17}, spin shuttling^{18,19} and SWAP-gate operations²⁰ have been proposed, all of which require control of electron spin transport across donors. In order to further investigate these transport protocols it is crucial to understand the spin dynamics at the two donor level. However, despite the plethora of theoretical knowledge on gate-defined semiconductor double quantum dots²¹⁻²³; double donor transport has not received as much attention.

Electron transport through donors has been shown to follow similar physics to that of quantum dots, for example, in the demonstration of a single-atom transistor⁹ and through donor chains showing Anderson-Mott transitions⁷. One of the most studied effects in quantum dots is Pauli spin blockade (PSB), which occurs at any equivalent charge transition to the $(1,1)\leftrightarrow(0,2)$, where (n_L, n_R) is the number of electrons on the left and right quantum dot. Whereas electron singlet states are allowed to tunnel between the dots, electron triplet states in the $(1,1)$ charge configuration cannot tunnel to the $(0,2)$ due to

the Pauli exclusion principle, thereby blocking the current. For this reason, in quantum dots, PSB has been vital for spin readout of singlet-triplet qubits⁵ and single electron spins³. Recently, PSB and coherent transport have been observed for double²⁴ and triple²⁵ phosphorus donor clusters in silicon.

In this paper we show how the interplay between the electron and nuclear spins of donor-based systems affects not only the charge transport, but also the spin transport. To understand the impact of these nuclear spins we use a master equation approach to conduct a comprehensive numerical analysis of electron transport through a double donor system. We investigate electron spin resonance (ESR) combined with PSB at low and high magnetic fields to manipulate and readout the electron spin states. Our most striking finding demonstrates that the presence of the quantised nuclear spin of the donors leads to a novel effect called nuclear spin blockade. Using this mechanism we propose a new spin readout protocol for the nuclear spins based on a measurement of the transport current. Finally, we analyse more realistic scenarios of inhomogeneous hyperfine interactions across the donors, as well as the case of multi-donor dots, which can be shown to be immune to nuclear spin blockade. Throughout the paper we neglect the dynamical behavior of the surrounding ²⁹Si nuclear spins present in natural silicon. This interaction is much smaller than the donor hyperfine interaction²⁶ and it has also been shown that Si:P devices can be fabricated in isotopically pure ²⁸Si where the absence of the ²⁹Si extends the electron coherence times²⁷.

II. TRANSPORT AT THE $(1,1)$ TO $(0,2)$ CHARGE TRANSITION

We consider two weakly coupled phosphorus donors in a silicon lattice (approximately 15–20 nm apart^{28,29}), P_L and P_R the left and right donor, respectively. Electrons are able to tunnel from in plane source to drain leads via

both donors as shown schematically in Fig. 1a. Describing the system is the Hamiltonian H ,

$$H = H_{ze} + H_{zn} + H_{tc} + H_{\Delta} + H_{hf}, \quad (1)$$

where H_{ze} and H_{zn} are the electron and nuclear Zeeman terms, H_{tc} is the tunnel coupling between the donor electrons, H_{Δ} is the energy detuning of the $|S_{02}\rangle$ state (singlet state with two electrons on a single donor nuclei) and H_{hf} is the hyperfine interaction, for further details see Appendix A and B. Throughout the paper we refer to the Hamiltonian in the singlet-triplet basis of the electrons with energies shown in Fig. 1b. By making a transformation from Hilbert space to Liouville space we incorporate incoherent processes that occur during spin transport³⁰ (see Appendix C). In doing so, tunnelling that occurs from the source at the rate Γ_L , to the donors and through to the drain at the rate Γ_R , are integrated with the coherent evolution of the system. Using this approach we can determine the spin and charge dynamics of the donor system during electron transport.

As a first demonstration of the effect of quantised nuclear spin states we study the electron transport from drain to source (reverse bias) in the infinite bias limit²¹ (reverse of Fig. 1a). In this scenario the charge cycle is $(0,1) \rightarrow (0,2) \rightarrow (1,1) \rightarrow (0,1)$, where (n_L, n_R) corresponds to the electron numbers on the left and right donor nuclei. In the case of quantum dots it has been shown that the current, I_{QD} , due to elastic tunneling as a function of the detuning, Δ , is given by a known expression involving the coherent and incoherent tunnel rates³¹,

$$I_{QD} = \frac{|e|\Gamma_L (\frac{t_c}{2})^2}{(\frac{\Gamma_R}{2})^2 + (\frac{t_c}{2})^2 (2 + \frac{\Gamma_L}{\Gamma_R}) + \Delta^2}, \quad (2)$$

where e is the electron charge and t_c is the tunnel coupling between the two dots. However, without an external magnetic (B_0) dependence, this equation will not account for any spin dynamics. For the reverse bias condition the left electron will tunnel to the source from any of the $(1,1)$ spin states giving rise to a current. The measurable current is then given by $I = |e|\Gamma_L P(1,1)$, where $P(1,1)$ is the probability of being in any $(1,1)$ charge configuration, including the electron triplet states $\{|T_{11}^+\rangle, |T_{11}^-\rangle\}$, see Appendix D for more details.

To investigate the effect the inclusion of these states has on electron transport we plot the difference in current, $\delta I = I - I_{QD}$, for $\Delta \geq 0$ in Fig. 2a. There is a peak in the current that can be seen to follow the point at which the electron exchange interaction, $J = \Delta/2 + \sqrt{(t_c/2)^2 + (\Delta/2)^2}$, ($t_c = 2$ GHz) is equal to the electron Zeeman energy, $\gamma_e B_0$. This is analogous to the canonical spin-funnel experiments⁵. At this value of detuning the hyperfine interaction mixes electron singlet-triplet states $|S_{02}\rangle \leftrightarrow |T_{11}^-\rangle$ via a nuclear spin flip, see Fig. 2b. This increase in the $(1,1)$ state population allows for the electron on P_L to tunnel off to the source giving rise to a larger current. In gate-defined quantum

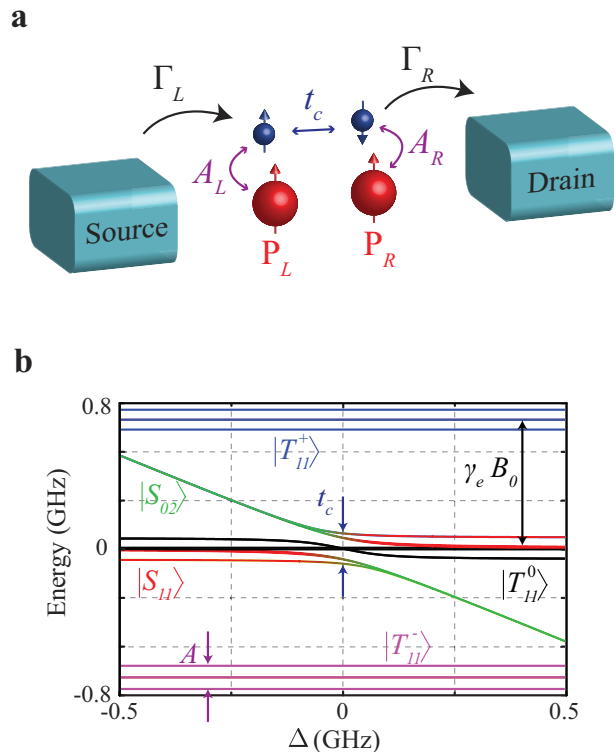


FIG. 1: **Electron transport through two weakly coupled phosphorus donors in silicon.** (a) A schematic representation of transport through a double donor system during PSB. Electrons can tunnel from the source to P_L and from P_R to the drain at rates Γ_L and Γ_R , respectively. The two donor electrons are coherently tunnel coupled at the rate t_c and have a contact hyperfine interaction with the nuclear spins, A_L and A_R with their respective nuclei. (b) Eigen energies of H around $\Delta=0$, between the $(1,1)$ and $(0,2)$ charge configurations at an external magnetic field of $B_0=25$ mT and with hyperfine interaction strength set to $A_L=A_R=A=117.53$ MHz. The electron triplet states, $|T_{11}^+\rangle$ (blue), $|T_{11}^0\rangle$ (black), and $|T_{11}^-\rangle$ (pink) are split by the Zeeman energy, $\gamma_e B_0$. The $|S_{02}\rangle$ (green) state is detuned from the $|S_{11}\rangle$ (red) with an anti-crossing at $\Delta=0$ due to a tunnel coupling set to $t_c = A$. The $(0,1)$ charge states are omitted for clarity.

dots this current peak is not observed since the large nuclear spin bath has a distribution of hyperfine strengths. Therefore, the position of this peak shown in Fig. 2a, will shift depending on the exact nuclear spin configuration and will be averaged out due to the fluctuating Overhauser field³².

For $\Delta \ll 0$ transport across the donors becomes energetically unfavourable as the electrons will remain in the $(1,1)$ region without first loading into the $(0,2)$ charge state, see Fig.1b. We therefore do not expect to see mixing between $|S_{02}\rangle \leftrightarrow |T_{11}^+\rangle$ and a current peak will not be observed.

III. NUCLEAR SPIN BLOCKADE

Next, we consider the transport cycle from source to drain (forward bias) in the infinite bias regime: $(0,1) \rightarrow (1,1) \rightarrow (0,2) \rightarrow (0,1)$ where we can expect PSB due to the large energy splitting of the $(0,2)$ electron singlet-triplet states³³. As a consequence, if the electrons are in any of the $(1,1)$ triplet states an electron on P_L cannot tunnel to P_R due the Pauli exclusion principle. Therefore, tunneling can only occur via the singlet states and the current is given solely by the $|S_{02}\rangle$ probability: $I = |e| \Gamma_R P(|S_{02}\rangle)$.

It has been shown; however, that by applying a continuous-wave ESR magnetic field PSB can be lifted by driving transitions within the $(1,1)$ electron triplet manifold, $\{|T_{11}^+\rangle, |T_{11}^-\rangle\} \leftrightarrow |T_{11}^0\rangle$ ^{3,34}. This applies when the tunnel coupling, t_c , is on the order A , hence, for the following analysis we set $t_c = A$. Importantly, any difference in the Larmor frequencies of the two electrons, $\delta\omega_e$, will

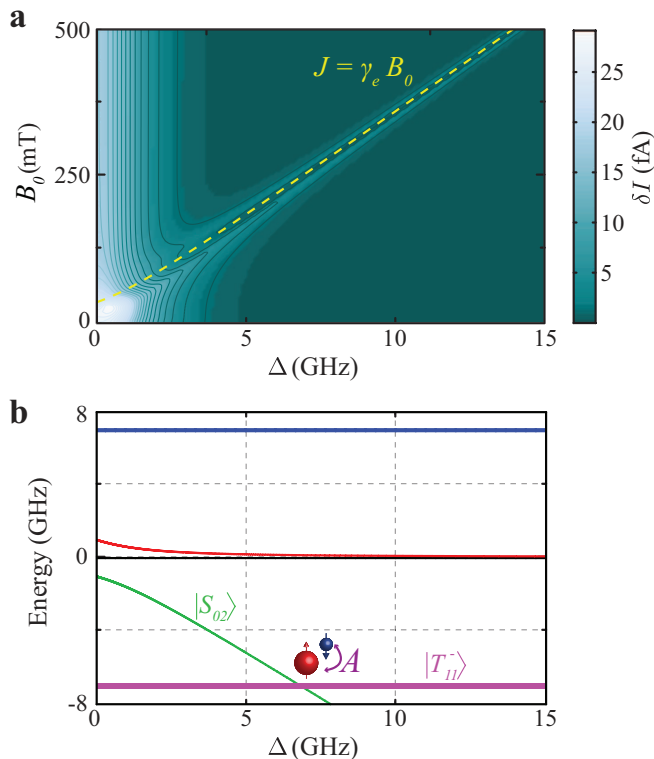


FIG. 2: **Electron transport through double donors from drain to source.** (a) The difference in current, δI , through a double donor as a function of detuning Δ , and external magnetic field, B_0 . The yellow line maps $J = \gamma_e B_0$ which follows a peak in δI due to the mixing between $|S_{02}\rangle \leftrightarrow |T_{11}^-\rangle$ (contour lines guide the eye). (b) Eigen energies of H at $B_0 = 250$ mT as a function of the detuning, showing the $|S_{02}\rangle \leftrightarrow |T_{11}^-\rangle$ anti-crossing. Here, H_{hf} allows for electron-nuclear spin flip-flops, increasing $P(1,1)$. The $(0,1)$ charge states are omitted for clarity. In this simulation $t_c = 2$ GHz, $A_L = A_R = A = 117.53$ MHz, $\Gamma_L = \Gamma_R = 100$ MHz.

result in $|T_{11}^0\rangle \leftrightarrow |S_{11}\rangle$ transitions³. The $|S_{11}\rangle$ state can in turn tunnel to $|S_{02}\rangle$ via the tunnel coupling t_c , allowing current to flow. In the presence of a homogeneous B_0 field $\delta\omega_e$ can only come from a difference in the nuclear spin orientation between the two donors.

We examine the spin transport by initialising in the $(0,1)$ charge configuration and preparing a fully mixed state in both the nuclear and electron spins states such that at $t = 0$, $\rho_0 = (|\uparrow_{01}\rangle\langle\uparrow_{01}| + |\downarrow_{01}\rangle\langle\downarrow_{01}|) \otimes \{N\}$ (normalisation omitted). We first let the system reach PSB after which a continuous wave ESR field is applied with strength B_1 and on resonance with the $(1,1)$ electron triplet manifold at the frequency³⁵,

$$\Omega = (\gamma_e - \gamma_n) B_0 + \frac{t_c}{4} + \frac{A_L - A_R}{2} + \frac{\sqrt{\frac{(A_L + A_R)^2}{4} + \frac{t_c^2}{4}}}{2}, \quad (3)$$

where γ_e and γ_n are the electron and nuclear gyromagnetic ratios, and A_L and A_R are the nuclear hyperfine interactions on P_L and P_R respectively.

At high magnetic fields, $B_0 \gtrsim 100$ mT, there is an initial peak in the current due to the tunneling of the electrons into the $(1,1)$ charge region, see Fig. 3a. In a time $\sim 0.1 \mu\text{s}$ PSB is reached and the current is blocked (Fig. 3b). After application of the ESR excitation the current initially spikes and coherent oscillations can be seen corresponding to electron spin rotations introducing singlet content at a frequency determined by the ESR field strength ($\gamma_e B_1 \sim 140$ MHz, Fig. 3c). The current quickly finds a steady state centred about the oscillations from the ESR driving. During this time, the nuclear spins are unaffected by the electron transport. Figure 3d shows the four nuclear spin state projections, $\{|\uparrow\uparrow\rangle, |\uparrow\downarrow\rangle, |\downarrow\uparrow\rangle, |\downarrow\downarrow\rangle\} = 0.25$.

In the case where the nuclear spins are not mixed and are instead in either $|\downarrow\downarrow\rangle$ or $|\uparrow\uparrow\rangle$ then $\delta\omega_e = 0$ and the application of ESR will not lift PSB. We refer to this effect as “nuclear spin blockade” since the current through the donors is being blocked as a result of the nuclear spin states. Nuclear spin blockade can be lifted by applying NMR to flip one of the nuclear spins so that the spins are anti-aligned. This creates a $\delta\omega_e = A$ allowing for transitions between $|T_{11}^0\rangle$ and $|S_{11}\rangle$.

At low magnetic fields, $B_0 < 100$ mT, the nuclear spin dynamics play a larger role in determining the current through the donors. Here the hyperfine interaction can cause electron-nuclear spin flip-flops ($|\uparrow\downarrow\rangle \leftrightarrow |\downarrow\uparrow\rangle$)^{36,37}. This process is seen to increase the nuclear spin $|\uparrow\uparrow\rangle$ and $|\downarrow\downarrow\rangle$ populations to ~ 0.3 whilst the system moves into PSB, see Fig. 3e. The flip-flop process is further amplified when ESR is applied causing the nuclear $|\uparrow\downarrow\rangle$ and $|\downarrow\uparrow\rangle$ populations approach zero. This can be understood as the ESR increasing the likelihood of the electron and nuclei to have opposite spin states in the $(1,1)$ charge region, that is, $|\uparrow\downarrow\rangle$ or $|\downarrow\uparrow\rangle$. The flip-flop process then becomes more likely to occur, eventually reducing the anti-aligned nuclear spin states probabilities since the electrons won't be blocked if the nuclear spins are in

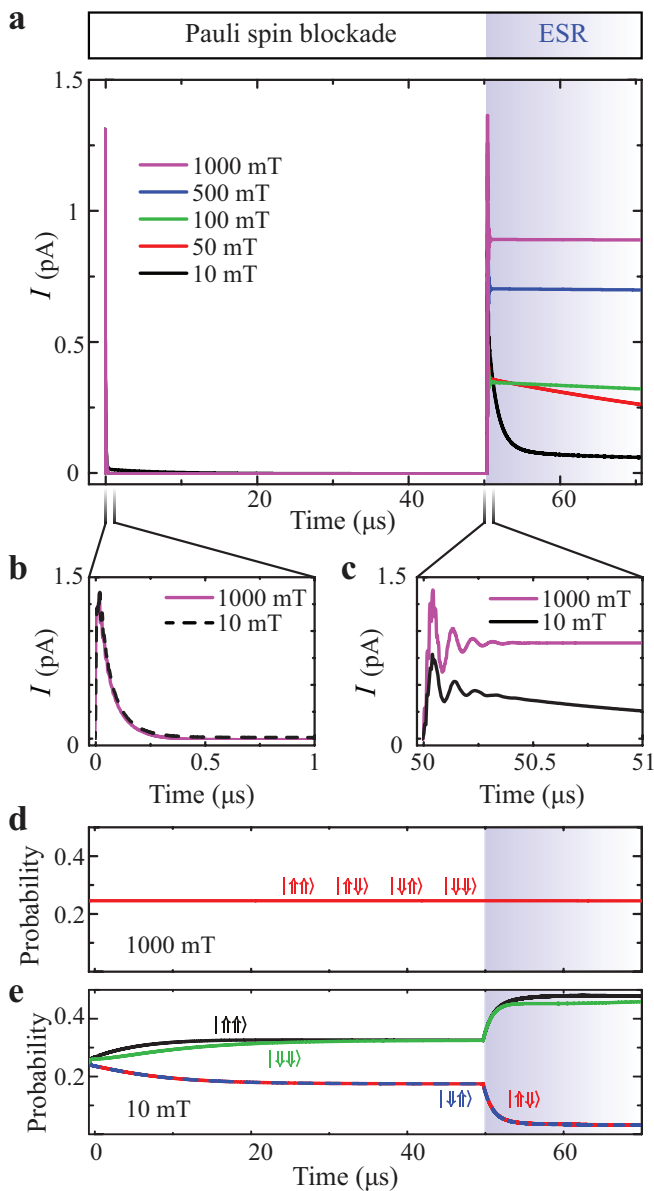


FIG. 3: **Current during Pauli spin blockade and nuclear spin blockade.** (a) The simulated current through two weakly coupled donors in transport for different external magnetic fields, B_0 . At $t=0$ the density operator is given by $\rho_0 = (|\uparrow_{01}\rangle\langle\uparrow_{01}| + |\downarrow_{01}\rangle\langle\downarrow_{01}|) \otimes \{N\}$ (normalisation omitted). (b) PSB is reached in $\sim 0.1 \mu\text{s}$ and the current drops to zero. (c) An ESR driving field is turned on after $50 \mu\text{s}$ affecting the spin of both donor electrons. For all values of B_0 there is an initial spike in the current corresponding to the lifting of PSB followed by coherent oscillations. (d) The nuclear spin state projections at $B_0=1000 \text{ mT}$ are unchanged during electron transport or after application of ESR due to the reduced electron-nuclear flip-flop events. (e) At $B_0=10 \text{ mT}$ the nuclear $|\uparrow\downarrow\rangle$ and $|\downarrow\uparrow\rangle$ approach zero probability (< 0.05 after $50 \mu\text{s}$), this is nuclear spin blockade. Simulations were carried out with $t_c = A_L = A_R = A = 117.53 \text{ MHz}$, $\Delta = 0$, $\Gamma_L = \Gamma_R = 100 \text{ MHz}$.

either $|\uparrow\downarrow\rangle$ or $|\downarrow\uparrow\rangle$. Consequently, this reduces the mixing between $|S_{11}\rangle$ and $|T_{11}^0\rangle$ since $\delta\omega_e \rightarrow 0$. Therefore, irrespective of the initial nuclear spin state, nuclear spin blockade cannot be lifted at low magnetic fields for double donor transport.

IV. NUCLEAR SPIN READOUT

In the same way that PSB has been used to perform single electron spin readout in electron transport³, we investigated if nuclear spin blockade can be used to perform readout of a single nuclear spin. Even at high magnetic fields nuclear spin blockade prevents current flow if the nuclear spin states are aligned ($|\uparrow\uparrow\rangle$ or $|\downarrow\downarrow\rangle$) and allows current to flow if they are anti-aligned ($|\uparrow\downarrow\rangle$ or $|\downarrow\uparrow\rangle$). Importantly, at high fields the nuclear spin states remain unaffected by the electron transport; therefore, it is possible to use nuclear spin blockade as a readout mechanism for the nuclear spin states.

The spin measurement protocol consists of 3 stages: initialisation, manipulation and readout, see Fig. 4a,b. We initialise in the (0,1) charge region by waiting for the T_1 of the nuclear spins, thereby preparing them in the ground state, $|\uparrow\uparrow\rangle$. This step would only need to be performed once since the measurement preserves the nuclear spin state. Therefore, the nuclear spin states can be tracked between successive measurements without the need to re-initialise. The manipulation step involves applying NMR to the P_L nuclear spin (which does not have an electron present) at a frequency $\gamma_n B_0$. Importantly, this will not effect the P_R nuclear spin due to the presence of the donor electron. The readout consists of moving to the (1,1) \rightarrow (0,2) transition and applying ESR to test the presence of nuclear spin blockade. If the nuclear spin on P_L is $|\downarrow\rangle$ then current will flow through the donors (Fig. 4c); however, if the nuclear spin is $|\uparrow\rangle$ then the current will be blocked (Fig. 4d). The current is also linearly proportional to the orientation of the nuclear spin; that is, if the total nuclear spin state is $(|\downarrow\uparrow\rangle + |\uparrow\downarrow\rangle)/\sqrt{2}$ then the current will be half that of the $|\downarrow\uparrow\rangle$ state, see Fig. 4e.

V. STARK SHIFT AND DONOR CLUSTERS

In this final section we extend the simulation work to examine non-idealised scenarios of Stark shifted contact hyperfine interactions and donor clusters (multi-donor quantum dots) in donor based transport, for example, in Ref.^{10,24,25}.

The electron wavefunction around a donor nuclei can be distorted by electric fields which changes the contact hyperfine interaction, known as the Stark effect^{11,38}. Due to the stray electric fields in the silicon crystal, e.g. from electronic gates or charges, it is most likely that two donors will naturally experience different hyperfine interactions. This inherent Stark shift is typically a few MHz

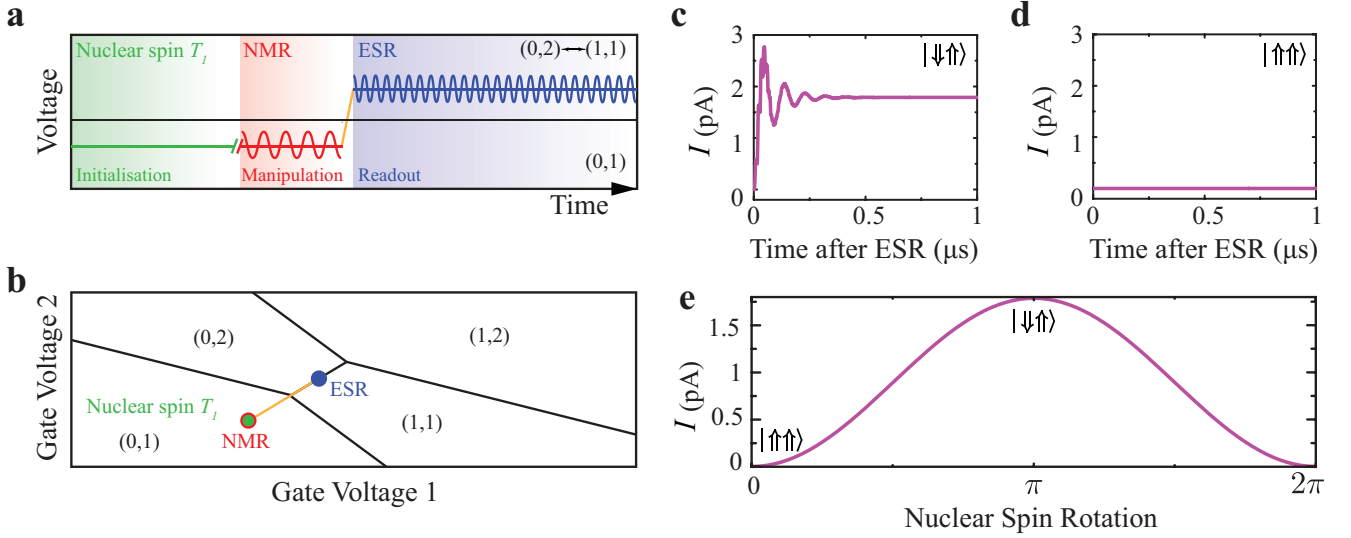


FIG. 4: **Nuclear spin readout using two weakly coupled donors in transport.** (a) Schematic representation of the proposed scheme for single nuclear spin readout of the P_L nuclear spin showing gate pulsing, NMR and ESR driving. The nuclear spins are initialised in $|\uparrow\uparrow\rangle$ by waiting T_1 . NMR can then be performed on P_L nuclei by driving at a frequency $\gamma_n B_0$, which does not effect the P_R nuclear spin due to the presence of the electron in the $(0,1)$ charge state. (b) The charge stability diagram for the double donor system with colors corresponding to movements in gate space for (a). Readout is performed by pulsing to the $(1,1)\leftrightarrow(0,2)$ transition and applying ESR. (c) If the nuclear spin state after NMR is $|\downarrow\uparrow\rangle$ then nuclear spin blockade does not occur. (d) However, if the spin state is $|\uparrow\uparrow\rangle$ then no current will flow due to nuclear spin blockade. (e) The current through the donors is linearly proportional to the spin down probability on P_L allowing different NMR rotations to be mapped using the magnitude of the current during readout. Here, $B_0=1000$ mT, $t_c=A_L=A_R=A=117.53$ MHz, $\Delta=0$, $\Gamma_L=\Gamma_R=100$ MHz.

in frequency³⁹ and will create a difference in the hyperfine interaction between the two donors, $\delta A_{LR}=|A_L - A_R|$.

Figure 5 shows the steady state current after PSB and ESR (as in Fig. 3a) for various magnetic fields and δA_{LR} values. The current increases with the magnetic field up to a certain field and interestingly there is an optimum B_0 for any given δA_{LR} . At high magnetic fields the cur-

rent decreases as δA_{LR} becomes larger. This is due to δA_{LR} decreasing $\delta\omega_e$ when the spins are anti-aligned, resulting in less $|S_{11}\rangle\leftrightarrow|T_{11}^0\rangle$ mixing and a lower current. At low magnetic fields the effect is reversed. Here, we are subject to nuclear spin blockade as previously discussed, however increasing δA_{LR} will only increase $\delta\omega_e$ resulting in a higher current.

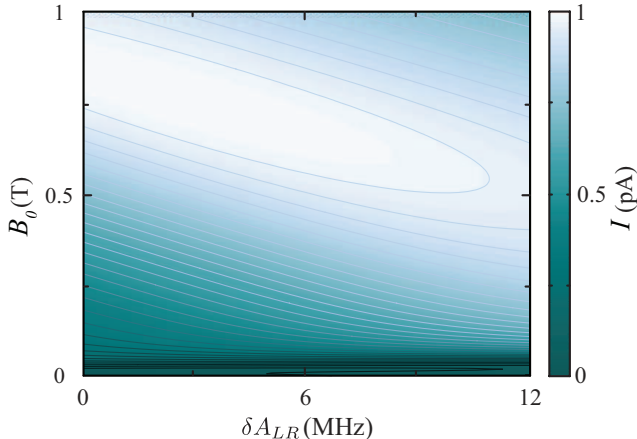


FIG. 5: **Effect of inhomogeneous contact hyperfine interactions.** At high magnetic fields where the nuclear spin dynamics are unaffected by the electron transport the effect of larger $\delta A_{LR}=|A_L - A_R|$ reduces the current. In order to achieve the largest current there is an optimum B_0 for any given δA_{LR} (contour lines guide the eye). Here, $\Delta=0$, $\Gamma_L=\Gamma_R=100$ MHz.

Using scanning tunneling microscopy (STM) hydrogen lithography it has been shown that donor clusters consisting of a small number of P atoms can be fabricated in Si that exhibit PSB²⁴. It is therefore possible to engineer a system consisting of a single donor and a two donor cluster in transport, essentially controlling the hyperfine interaction at the atomic scale. Now, in this system the electrons will always experience a $\delta\omega_e$ across the two dots, ensuring there is substantial mixing ($\gtrsim A$) between the $|T_{11}^0\rangle$ and $|S_{11}\rangle$ states to lift PSB. This can be seen if we consider the 8 possible nuclear configurations: $\{N_{1P/2P}\}=\{|\uparrow\rangle|\uparrow\rangle, |\uparrow\rangle|\uparrow\downarrow\rangle, |\uparrow\rangle|\downarrow\uparrow\rangle, |\uparrow\rangle|\downarrow\downarrow\rangle, |\downarrow\rangle|\uparrow\uparrow\rangle, |\downarrow\rangle|\uparrow\downarrow\rangle, |\downarrow\rangle|\downarrow\uparrow\rangle, |\downarrow\rangle|\downarrow\downarrow\rangle\}$, where the first term is the spin state for P_L and the second term with a two nuclear spin state is for $2P_R$.

We simulate the current through a single donor (P_L) and two donor cluster ($2P_R$) in Fig. 6a at different magnetic fields with the initial state $\rho_0=(|\uparrow_{01}\rangle\langle\uparrow_{01}| + |\downarrow_{01}\rangle\langle\downarrow_{01}|) \otimes \{N_{1P/2P}\}$ at $t=0$. With this single and two donor cluster scenario, the nuclear spins take longer to reach a steady state configuration despite the electron spins reaching PSB in the same time scale as the single donor case, Fig. 6b. As a consequence we simulate the dynamics here for much longer.

During ESR excitation the current is seen to oscillate

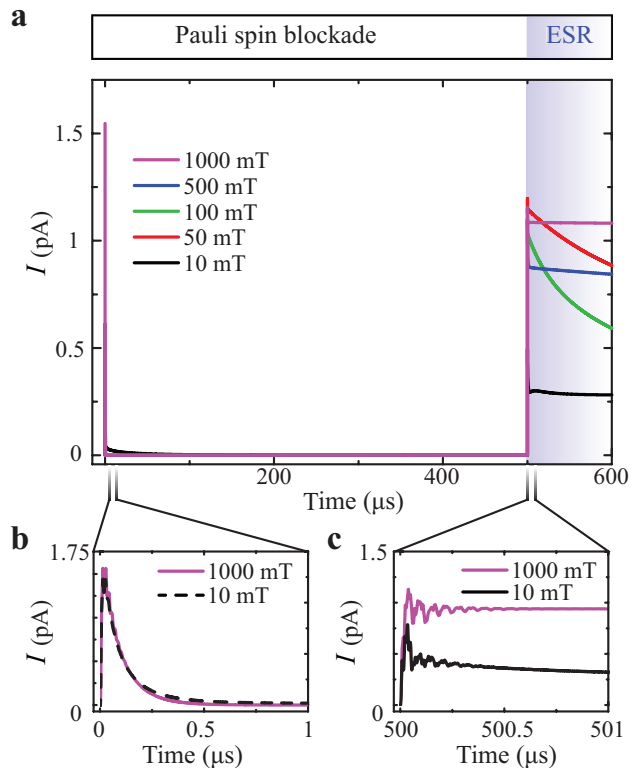


FIG. 6: **Current through a single donor and a two-donor cluster.** (a) Simulated electron transport for a single donor (P_L) and two donor cluster ($2P_R$) at different magnetic fields showing the absence of nuclear spin blockade. The initial density operator was $\rho_0=(|\uparrow_{01}\rangle\langle\uparrow_{01}| + |\downarrow_{01}\rangle\langle\downarrow_{01}|) \otimes \{N_{1P/2P}\}$ (normalisation omitted). (b) PSB is reached on a similar time scale for two single donors in transport for all magnetic fields. (c) After $500 \mu\text{s}$ an ESR driving field is applied to both electron spins. At low magnetic fields the current reaches a steady state but it does not decay to zero. The absence of decay in the current at low magnetic fields indicates that nuclear spin blockade is no longer present. At intermediate magnetic fields (50 mT and 100 mT) there is a decay in the current; however, the final steady state current is larger than that obtained for two single donors in transport. In this simulation, $t_c=A_L=A_R=117.53$ MHz, $\Delta=0$, $\Gamma_L=\Gamma_R=100$ MHz.

with a beating due to the different hyperfine interactions experienced by each electron, see Fig. 6c. For all magnetic field strengths, the current is higher than it was in the single donor cases. Importantly, even at low magnetic fields, and in contrast to the single donor dynamics (Fig. 3a), the current does not decay to zero. Instead, it finds a steady state solution centered around the coherent oscillations indicating that nuclear spin blockade is no longer present.

VI. SUMMARY

We have developed a numerical model to investigate electron spin transport through donors in silicon. Our findings show that there are surprising effects that arise due to the quantised nature of the donor nuclei. We show

how it is possible to map out the electron exchange interaction using simple transport measurements and predict a new current blockade mechanism as a consequence of nuclear spin dynamics. This is in contrast to other systems such as GaAs double quantum dots where large fluctuating nuclear spin baths averages out the quantum nature of the nuclear spins and these effects are not observed.

Importantly, we find that for low magnetic fields, $B_0 < 100$ mT, where long electron T_1 times⁴⁰ and faster ESR rotations are possible, nuclear spin blockade prevents the transfer of the electron spins across the donors. Therefore, electron spin readout can only be performed at high magnetic fields; in which, the nuclear spin states are initialised in $|\uparrow\downarrow\rangle$ or $|\downarrow\uparrow\rangle$ otherwise $\delta\omega_e=0$ and there will be no $|S_{11}\rangle \leftrightarrow |T_{11}^0\rangle$ mixing. In addition, we demonstrate that there is an optimum B_0 field for a given Stark shift across the donors to achieve the maximum current after ESR driving.

Interestingly, we show how nuclear spin blockade can be utilised as a new readout mechanism for nuclear spins. This method, which only requires electron transport measurements and removes the need for traditional charge sensors will be a useful experimental tool for probing multi-donor interactions. The nuclear spin coherence times can be measured during electron shuttling which is critical for many proposed spin transport protocols^{18,19}.

Finally, we demonstrate that for electron spin transport experiments where nuclear spin blockade is undesir-

able, multi-donor clusters can be used since they allow for lifting of PSB even at low magnetic fields. Advances in fabrication technologies, in particular STM lithography, offers the ability to tailor hyperfine interactions at the atomic scale for absolute control over the combined electron-nuclear spin system.

Our results provide important insights into the complex spin dynamics in double donor systems. Such an understanding is necessary for two-qubit interactions³⁵ and spin transport protocols in multi-donor chains⁴¹ for scalable solid-state quantum computing architectures¹².

Acknowledgments We thank T. L. Keevers and J. G. Keizer for helpful discussions. This research was conducted by the Australian Research Council Centre of Excellence for Quantum Computation and Communication Technology (project no. CE110001027) and the US National Security Agency and US Army Research Office (contract no. W911NF-08-1-0527). M.Y.S. acknowledges an ARC Laureate Fellowship.

Appendix A: Hamiltonian definition

The Hamiltonian for exchange coupled donors including hyperfine, H_{hf} and electrical detuning, H_Δ written in the singlet-triplet basis of the donor electrons is given by,

$$\begin{aligned}
 H_{ST} &= H_{ze} + H_{zn} + H_{tc} + H_\Delta + H_{hf} \\
 H_{ze} &= \gamma_e B_0 (|T_{11}^+\rangle\langle T_{11}^+| - |T_{11}^-\rangle\langle T_{11}^-|) + \frac{\gamma_e}{2} B_0 (|\uparrow_{01}\rangle\langle\uparrow_{01}| - |\downarrow_{01}\rangle\langle\downarrow_{01}|) \\
 H_{zn} &= \gamma_n B_0 (|\downarrow\downarrow\rangle\langle\downarrow\downarrow| - |\uparrow\uparrow\rangle\langle\uparrow\uparrow|) \\
 H_{tc} &= \frac{t_c}{2} (|S_{11}\rangle\langle S_{02}| + |S_{02}\rangle\langle S_{11}|) \\
 H_\Delta &= -\Delta |S_{02}\rangle\langle S_{02}| \\
 H_{hf} &= A_L \vec{S}_L^{(1,1)} \cdot \sum_{i_L} \vec{I}_{i_L} + A_R \vec{S}_R^{(1,1)} \cdot \sum_{i_R} \vec{I}_{i_R} + A_R \vec{S}_1 \cdot \sum_{i_R} \vec{I}_{i_R},
 \end{aligned} \tag{A1}$$

where in the Zeeman term, $\vec{B}_0 = (0, 0, B_0)$ and the gyromagnetic ratios of the electron and nuclear spin states are $\gamma_e = 28.024$ GHz/T and $\gamma_n = 17.235$ MHz/T which will define the respective resonance conditions during either electron or nuclear spin excitation. Throughout the article we assume that the donors are in the weak coupling regime where valley and orbital effects are negligible.

The terms $\vec{S}_L^{(1,1)}$ and $\vec{S}_R^{(1,1)}$ are the electron spin operators for the (1,1) charge state and \vec{I}_{i_L} and \vec{I}_{i_R} are the nuclear spin operators for P_L and P_R (with donor numbers $i_L = i_R = 1$ for single donors). To account for tunneling out of the $|S_{02}\rangle$ state to the drain we have included

the single electron states $|\uparrow_{01}\rangle$ and $|\downarrow_{01}\rangle$ which represent the spin states of the electron in the (0,1) charge state³⁴. For these single electron states, the system has three particles, two nuclei and one electron spin such that the hyperfine coupling is only between the electron spin, \vec{S}_1 , and the second donor nuclei, \vec{I}_{i_R} . By considering the two donor nuclei quantum mechanically we can obtain the full system spin dynamics.

In total our Hamiltonian is spanned by $\{E\} \otimes \{N\}$ where $\{N\}$ represents the nuclear subspace of states $\{|\uparrow\uparrow\rangle, |\uparrow\downarrow\rangle, |\downarrow\uparrow\rangle, |\downarrow\downarrow\rangle\}$ and $\{E\}$ the electron subspace consisting of $\{|T_{11}^i\rangle, |S_{11}\rangle, |S_{02}\rangle, |\uparrow_{01}\rangle, |\downarrow_{01}\rangle\}$, where $i =$

$+, 0, -$.

To include incoherent terms we make use of a technique commonly used in the ESR/NMR community^{30,42,43}, which involves transforming from Hilbert space (\mathcal{H}_n) to a higher dimensional space—Liouville space, \mathcal{L}_{n^2} . The incoherent processes can then be gathered into the dissipator superoperator, $\hat{\mathcal{D}}$ in \mathcal{L}_{n^2} that can model non-trace preserving decoherence processes without the need of finding the operators in \mathcal{H}_n .

Appendix B: Rotating wave approximation

The ESR addition to the Hamiltonian (Eq. A1) is

$$H_{ESR} = \gamma_e B_{ac}^{esr} \cos(\Omega t) (S_{L(x)}^{(1,1)} + S_{R(x)}^{(1,1)} + S_{1(x)}), \quad (\text{B1})$$

where we chose a realistic $B_{ac}^{esr}=1$ mT as the microwave magnetic field strength^{3,39}, Ω its frequency and $\{S_{L(x)}^{(1,1)}, S_{R(x)}^{(1,1)}, S_{1(x)}\}$ are the electron x -spin operators for the (1,1) and (0,1) charge state respectively. To remove the time-dependence of the ESR field we can make a transformation from the laboratory frame to the rotating frame of the Larmor frequency (ω_e) of the electron spins. This is simply a rotation about z by an angle $\theta=\omega_e t$. We can then remove the faster rotating terms by making the rotating wave approximation. This transforms the Hamiltonian according to

$$H_{rot} = R_z^\theta H R_z^{\theta\dagger} - R_z^\theta \frac{dR_z^{\theta\dagger}}{dt}. \quad (\text{B2})$$

This amounts to a two term addition to the Hamiltonian

$$H_{rot} = H + H_1 - F, \quad (\text{B3})$$

where H is the non-rotating Hamiltonian, $H_1=\gamma_e B_1(S_{L(x)}^{(1,1)}+S_{R(x)}^{(1,1)}+S_{1(x)})$ and $F=\Omega\sigma_z$. H_1 contains the ESR driving terms and F is the correction term due to the approximation ($B_1=B_{ac}^{esr}/2$ and σ_z is the z operator for the entire Hilbert space).

Appendix C: Liouville Space

To incorporate decoherence and relaxation into the time evolution of the density operator, a master equation approach can be used. The problem is treated in a higher-dimensional space, known as Liouville space, \mathcal{L}_{n^2} . The master equation in Liouville space is given by⁴⁴,

$$\frac{d|\rho\rangle}{dt} = \frac{i}{\hbar} \hat{\mathcal{L}}|\rho\rangle + \hat{\mathcal{D}}|\rho\rangle = \hat{G}|\rho\rangle. \quad (\text{C1})$$

Importantly, the density operator is now a vector of length n^2 , which is operated upon by the Liouvillian

superoperator, $\hat{\mathcal{L}}=\mathbb{I}\otimes H-H\otimes\mathbb{I}$ and the dissipator superoperator $\hat{\mathcal{D}}$ representing incoherent terms. When \hat{G} is time-independent Eq. C1 has the solution,

$$|\rho(t)\rangle = e^{\hat{G}t}|\rho(0)\rangle. \quad (\text{C2})$$

Appendix D: The dissipator superoperator

The dissipator superoperator term contains the tunnel rates between the source and P_L , the drain and P_R , Γ_L and Γ_R respectively. The elements of $\hat{\mathcal{D}}$ that contain these rates are determined by the effect they have on the system^{2,34}.

Two electron transport cycles were studied in this paper, for the first case: $(0,1)\rightarrow(0,2)\rightarrow(1,1)\rightarrow(0,1)$, the electrons are tunneling from the drain through the dots to the source. The diagonal dissipator elements in this scenario are,

$$\begin{aligned} \hat{\mathcal{D}}[|T_{11}^+\rangle] &= -\Gamma_L |\rho_{T_{11}^+ T_{11}^+}\rangle \\ \hat{\mathcal{D}}[|T_{11}^0\rangle] &= -\Gamma_L |\rho_{T_{11}^0 T_{11}^0}\rangle \\ \hat{\mathcal{D}}[|S_{11}\rangle] &= -\Gamma_L |\rho_{S_{11} S_{11}}\rangle \\ \hat{\mathcal{D}}[|T_{11}^-\rangle] &= -\Gamma_L |\rho_{T_{11}^- T_{11}^-}\rangle \\ \hat{\mathcal{D}}[|S_{02}\rangle] &= \Gamma_R (|\rho_{\uparrow_{01}\uparrow_{01}}\rangle + |\rho_{\downarrow_{01}\downarrow_{01}}\rangle) \\ \hat{\mathcal{D}}[|\uparrow_{01}\rangle] &= \Gamma_L |\rho_{T_{11}^+ T_{11}^+}\rangle + \frac{\Gamma_L}{2} (|\rho_{T_{11}^0 T_{11}^0}\rangle + |\rho_{S_{11} S_{11}}\rangle) \\ &\quad - \Gamma_R |\rho_{\uparrow_{01}\uparrow_{01}}\rangle \\ \hat{\mathcal{D}}[|\downarrow_{01}\rangle] &= \Gamma_L |\rho_{T_{11}^- T_{11}^-}\rangle + \frac{\Gamma_L}{2} (|\rho_{T_{11}^0 T_{11}^0}\rangle + |\rho_{S_{11} S_{11}}\rangle) \\ &\quad - \Gamma_R |\rho_{\downarrow_{01}\downarrow_{01}}\rangle, \end{aligned} \quad (\text{D1})$$

where $|\rho_{jk}\rangle$ indicates the the density operator element that $\hat{\mathcal{D}}[j]$ acts upon. The off-diagonal elements between states j and k are

$$\hat{\mathcal{D}}[|j\rangle|k\rangle] = -\frac{\Gamma_{j,k}}{2} |\rho_{jk}\rangle, \quad (\text{D2})$$

here $\Gamma_{j,k}=\Gamma_R$ (Γ_L) if $j, k=|\uparrow_{01}\rangle$ or $|\downarrow_{01}\rangle$ ($|T_{11}^i\rangle, |S_{11}\rangle$); otherwise, it is zero. The tunneling rates account for the loss of coherence between the states j and k during transport and must be included to ensure positivity of the density operator.

The current through donors is given by the probability of the system to be in the (1,1) charge configuration multiplied by the tunnel rate from P_L to the drain

$$\begin{aligned} I &= |e|\Gamma_L (|\rho_{T_{11}^+ T_{11}^+}\rangle + |\rho_{T_{11}^0 T_{11}^0}\rangle + |\rho_{T_{11}^- T_{11}^-}\rangle + |\rho_{S_{11} S_{11}}\rangle) \\ &= |e|\Gamma_L (P(T_{11}^+) + P(T_{11}^0) + P(T_{11}^-) + P(S_{11})) \\ &= |e|\Gamma_L P(1,1). \end{aligned} \quad (\text{D3})$$

For the electron transport cycle: $(0,1) \rightarrow (1,1) \rightarrow (0,2) \rightarrow (0,1)$, the electrons are tunneling from the source through the donors to the drain. So here the dissipator elements are essentially reversed

$$\begin{aligned}
\hat{\mathcal{D}}[|T_{11}^+\rangle] &= \frac{\Gamma_L}{2} |\rho_{\uparrow 01 \uparrow 01}\rangle \\
\hat{\mathcal{D}}[|T_{11}^0\rangle] &= \frac{\Gamma_L}{4} (|\rho_{\uparrow 01 \uparrow 01}\rangle + |\rho_{\downarrow 01 \downarrow 01}\rangle) \\
\hat{\mathcal{D}}[|S_{11}\rangle] &= \frac{\Gamma_L}{4} (|\rho_{\uparrow 01 \uparrow 01}\rangle + |\rho_{\downarrow 01 \downarrow 01}\rangle) \\
\hat{\mathcal{D}}[|T_{11}^-\rangle] &= \frac{\Gamma_L}{2} |\rho_{\downarrow 01 \downarrow 01}\rangle \\
\hat{\mathcal{D}}[|S_{02}\rangle] &= -\Gamma_R |\rho_{S_{02} S_{02}}\rangle \\
\hat{\mathcal{D}}[|\uparrow_{01}\rangle] &= \frac{\Gamma_R}{2} |\rho_{S_{02} S_{02}}\rangle - \Gamma_L |\rho_{\uparrow 01 \uparrow 01}\rangle \\
\hat{\mathcal{D}}[|\downarrow_{01}\rangle] &= \frac{\Gamma_R}{2} |\rho_{S_{02} S_{02}}\rangle - \Gamma_L |\rho_{\downarrow 01 \downarrow 01}\rangle,
\end{aligned} \tag{D4}$$

where now, for the off-diagonal elements, $\Gamma_{j,k} = \Gamma_R$ (Γ_L)

if $j, k = |S_{02}\rangle$ ($|\uparrow_{01}\rangle$ or $|\downarrow_{01}\rangle$); otherwise, it is zero.

To determine the current through the donors we calculate the probability for the system to be in $|S_{02}\rangle$ multiplied by the tunnel rate from P_R to the drain³²

$$I = |e| \Gamma_R |\rho_{S_{02} S_{02}}\rangle = |e| \Gamma_R P(|S_{02}\rangle). \tag{D5}$$

Throughout the paper we choose $\Gamma_L = \Gamma_R = 100$ MHz, such that it is less than A so that the hyperfine interaction has time to mix the electron states but still large enough to give an appreciable current through the donors.

-
- ¹ A. C. Johnson, J. R. Petta, C. M. Marcus, M. P. Hanson, and A. C. Gossard. Singlet-triplet spin blockade and charge sensing in a few-electron double quantum dot. *Nature*, 435: 925–928, 2005.
- ² F. H. L. Koppens, J. A. Folk, J. M. Elzerman, R. Hanson, L. H. Williems van Beveran, I. T. Vink, H. P. Tranitz, W. Wegscheider, L. P. Kouwenhoven, and L. M. K. Vandersypen. Control and detection of singlet-triplet mixing in a random nuclear field. *Science*, 309:1346–1350, 2005.
- ³ F. H. L. Koppens, C. Buizert, K. J. Tielrooij, I. T. Vink, K. C. Nowack, T. Meunier, L. P. Kouwenhoven, and L. M. K. Vandersypen. Driven coherent oscillations of a single electron spin in a quantum dot. *Nature*, 442:766–771, 2006.
- ⁴ K. C. Nowack, M. Shafiei, M. Laforest, G. E. D. K. Prawiroatmodjo, L. R. Schreiber, C. Recihl, W. Wegscheider, and L. M. K. Vandersypen. Single-shot correlations and two-qubit gate of solid-state spins. *Science*, 333:1269–1272, 2011.
- ⁵ J. R. Petta, A. C. Johnson, J. M. Taylor, E. A. Laird, A. Yacoby, M. D. Lukin, C. M. Marcus, M. P. Hanson, and A. C. Gossard. Coherent manipulation of coupled electron spins in semiconductor quantum dots. *Science*, 309:2180–2184, 2005.
- ⁶ M. J. A. Schuetz, E. M. Kessler, L. M. K. Vandersypen, J. I. Cirac, and G. Giedke. Nuclear spin dynamics in double quantum dots: Multistability, dynamical polarisation, criticality, and entanglement. *Phys. Rev. B*, 89:195310, 2014.
- ⁷ E. Prati, M. Hori, F. Guagliardo, G. Ferrari, and T. Shinada. Anderson-mott transition in arrays of a few dopant atoms in a silicon transistor. *Nature Nanotech.*, 7:443–447, 2012.
- ⁸ M. F. Gonzalez-Zalba, A. Saraiva, M. J. Calderon, D. Heiss, B. Koiller, and A. J. Ferguson. An exchange-coupled donor molecule in silicon. *Nano Lett.*, 14:5672–5676, 2014.
- ⁹ M. Fuechsle, J. A. Miwa, S. Mahapatra, H. Ryu, S. Lee, O. Warschkow, L. C. L. Hollenberg, G. Klimeck, and M. Y. Simmons. A single-atom transistor. *Nature Nanotech.*, 7: 242–246, 2012.
- ¹⁰ B. Weber, S. Mahapatra, T. F. Watson, and M. Y. Simmons. Engineering independent electrostatic control of atomic-scale (~ 4 nm) silicon double quantum dots. *Nano Lett.*, 12:4001–4006, 2012.
- ¹¹ H. Buch, S. Mahapatra, R. Rahman, A. Morello, and M. Y. Simmons. Spin readout and addressability of phosphorous-donor clusters in silicon. *Nature Commun.*, 4:2017, 2013.
- ¹² L. C. L. Hollenberg, A. D. Greentree, A. G. Fowler, and C. J. Wellard. Two-dimensional architectures for donor-based quantum computing. *Phys. Rev. B*, 74:045311, 2006.
- ¹³ S. Bose. Quantum communication through an unmodulated spin chain. *Phys. Rev. Lett.*, 91:207901, 2003.
- ¹⁴ S. Bose. Quantum communication through spin chain dynamics: an introductory overview. *Contemp. Phys.*, 48: 13–30, 2007.
- ¹⁵ A. Kay. Perfect, efficient, state transfer and its applications as a constructive tool. *Int. J. Quantum Inf.*, 8:641, 2010.
- ¹⁶ R. Rahman, S. H. Park, J. H. Cole, A. D. Greentree, R. P. Muller, G. Klimeck, and L. C. L. Hollenberg. Atomistic simulations of adiabatic coherent electron transport in triple donor systems. *Phys. Rev. B*, 80:035302, 2009.
- ¹⁷ R. Rahman, R. P. Muller, J. E. Levy, M. S. Carroll, G. Klimeck, A. D. Greentree, and L. C. L. Hollenberg. Coherent electron transport by adiabatic passage in an imperfect donor chain. *Phys. Rev. B*, 82:155315, 2010.
- ¹⁸ J. I. Cirac and P. Zoller. A scalable quantum computer with ions in an array of microtraps. *Nature*, 404:579–581, 2000.
- ¹⁹ A. J. Skinner, M. E. Davenport, and B. E. Kane. Hydrogenic spin quantum computing in silicon: A digital approach. *Phys. Rev. Lett.*, 90:087901, 2003.
- ²⁰ D. Loss and D. P. DiVincenzo. Quantum computation with quantum dots. *Phys. Rev. A*, 57:120–126, 1998.

- ²¹ W. G. van der Wiel, S. De Franceschi, J. M. Elzerman, T. Fujisawa, S. Tarucha, and L. P. Kouwenhoven. Electron transport through double quantum dots. *Rev. Mod. Phys.*, 75:1–22, 2003.
- ²² J. M. Taylor, J. R. Petta, A. C. Johnson, A. Yacoby, C. M. Marcus, and M. D. Lukin. Relaxation, dephasing, and quantum control of electron spins in double quantum dots. *Phys. Rev. B*, 76:035315, 2007.
- ²³ R. Hanson, L. P. Kouwenhoven, J. R. Petta, S. Tarucha, and L. M. K. Vandersypen. Spins in few-electron quantum dots. *Rev. Mod. Phys.*, 79:1217–1265, 2007.
- ²⁴ B. Weber, Y. H. Matthias Tan, S. Mahapatra, T. F. Watson, H. Ryu, R. Rahman, L. C. L. Hollenberg, G. Kilmeck, and M. Y. Simmons. Spin blockade and exchange in Coulomb-confined silicon double quantum dots. *Nature Nanotech.*, 9:430–435, 2014.
- ²⁵ T. Watson, B. Weber, J. A. Miwa, S. Mahapatra, R. M. P. Heijen, and M. Y. Simmons. Transport in asymmetrically coupled donor-based silicon triple quantum dots. *Nano Lett.*, 14:1830–1835, 2014.
- ²⁶ J. Schliemann, A. Khaetskii, and D. Loss. Electron spin dynamics in quantum dots and related nanostructures due to hyperfine interaction with nuclei. *J. Phys.: Condens. Matter*, 15:R1809–R1833, 2003.
- ²⁷ J. T. Muhonen, J. P. Dehollain, A. Laucht, F. E. Hudson, R. Kalra, T. Sekiguchi, K. M. Itoh, D. N. Jamieson, J. C. McCallum, A. S. Dzurak, and A. Morello. Storing quantum information for 30 seconds in a nanoelectronic device. *Nature Nanotech.*, 9:986–991, 2014.
- ²⁸ B. Koiller, X. Hu, and S. Das Sarma. Exchange in silicon-based quantum computer architecture. *Phys. Rev. Lett.*, 88:027903, 2002.
- ²⁹ C. J. Wellard, L. C. L. Hollenberg, F. Pariosoli, L. M. Kettle, H.-S. Goan, J. A. L. McIntosh, and D. N. Jamieson. Electron exchange coupling for single-donor solid-state spin qubits. *Phys. Rev. B*, 68:195209, 2003.
- ³⁰ R. R. Ernst, G. Bodenhausen, and A. Wokaun. *Principles of Nuclear Magnetic Resonance in One and Two Dimensions*. Oxford University Press, 1987.
- ³¹ Yu. V. Nazarov. Quantum interference, tunnel junctions and resonant tunneling interferometer. *Physica B*, 189:57–69, 1993.
- ³² O. N. Jouravlev and Y. V. Nazarov. Electron transport in a double quantum dot governed by a nuclear magnetic field. *Phys. Rev. Lett.*, 96:176804, 2006.
- ³³ K. Ono, D. G. Austing, Y. Tokura, and Y. Tarucha. Current rectification by Pauli exclusion in a weakly coupled double quantum dot system. *Science*, 297:1313–1317, 2002.
- ³⁴ F. H. L. Koppens, C. Buizert, I. T. Vink, K. C. Nowack, T. Meunier, L. P. Kouwenhoven, and L. M. K. Vandersypen. Detection of single electron spin resonance in a double quantum dot. *J. Appl. Phys.*, 101:081706, 2007.
- ³⁵ R. Kalra, A. Laucht, C. D. Hill, and A. Morello. Robust two-qubit gates for donors in silicon controlled by hyperfine interactions. *Phys. Rev. X*, 4:021044, 2014.
- ³⁶ D. R. McCamey, J. van Tol, G. W. Morely, and C. Boehme. Fast nuclear spin hyperpolarization of phosphorus in silicon. *Phys. Rev. Lett.*, 102:027601, 2009.
- ³⁷ D. R. McCamey, J. van Tol, G. W. Morely, and C. Boehme. Electronic spin storage in an electrically readable nuclear spin memory with a lifetime > 100 seconds. *Science*, 330:1652–1656, 2010.
- ³⁸ F. R. Bradbury, A. M. Tyryshkin, G. Sabouret, J. Bokor, T. Schenkel, and S. A. Lyon. Stark tuning of donor electron spins in silicon. *Phys. Rev. Lett.*, 97:176404, 2006.
- ³⁹ J. J. Pla, K. Y. Tan, J. P. Dehollain, W. H. Lim, J. J. L. Morton, D. N. Jamieson, A. S. Dzurak, and A. Morello. A single-atom electron spin qubit in silicon. *Nature*, 489:541–545, 2012.
- ⁴⁰ A. Morello, J. J. Pla, F. A. Zwanenburg, K. W. Chan, K. Y. Tan, H. Huebl, M. Mottonen, C. D. Nugroho, C. Yang, J. A. van Donkelaar, A. D. C. Alves, D. N. Jamieson, C. C. Escott, L. C. L. Hollenberg, R. G. Clark, and A. S. Dzurak. Single-shot readout of an electron spin in silicon. *Nature*, 467:687–691, 2010.
- ⁴¹ S. Oh, Y.-P. Shim, J. Fei, M. Friessen, and X. Hu. Resonant adiabatic passage with three qubits. *Phys. Rev. A*, 87:022332, 2013.
- ⁴² J. Jeener. Superoperators in magnetic resonance. *Adv. Magn. Opt. Res.*, 10:1–51, 1982.
- ⁴³ C. L. Mayne. Liouville equation of motion. *eMagRes.*, 2007.
- ⁴⁴ M. E. Limes, J. Wang, W. J. Baker, S.-Y. Lee, B. Saam, and C. Boehme. Numerical study of spin-dependent transition rates within pairs of dipolar and exchange coupled spins with $s = \frac{1}{2}$ during magnetic resonant excitation. *Phys. Rev. B*, 87:165204, 2013.